ACS APPLIED MATERIALS & INTERFACES

www.acsami.org

Research Article

3-Methylthiophene: A Sustainable Solvent for High-Performance Organic Solar Cells

Tingfu Liu, Jiaqing Liu, Yiming Li, Xiaomei Gao, Meng Wang,* Zehua Zhou,* Haiyan He,* Qing Zhang, Lijun Li, Huajie Huang, Jinchong Xiao, and Chang-Qi Ma

Cite This: *ACS Appl. Mater. Interfaces* 2024, 16, 50916−50925

Read Online

ACCESS | Metrics & More | Article Recommendations | Supporting Information

ABSTRACT: The use of harmful halogenated or aromatic solvents such as chloroform (CF), chlorobenzene (CB), and *o*-xylene (*o*-XY) is one of the greatest barriers to the industrial-scale manufacturing of high-performance organic solar cells (OSCs). Therefore, it is necessary to eliminate the effects of these solvents to ensure practical feasibility of OSCs. We found that the anthracene-terminated polymer donor and small-molecule acceptor BO-4Cl had good solubility in 3-methylthiophene (3-MeT). There were no toxicity labels in the SDS and exposure control limits for 3-MeT. An overall power conversion efficiency of 16.87% was achieved by using 3-MeT as the solvent for solar cell fabrication, which was higher than that of the cells made from CF (16.18%) and *o*-XY (15.69%). The best OSC based on PM6:D18:L8-BO and fabricated with 3-MeT exhibited a high PCE of 18.13%, which is one of the highest values for cells fabricated from halogen-free solvents. These results indicate that 3-MeT is an eco-friendly and low-toxicity solvent for the sustainable fabrication of the OSC active layer.

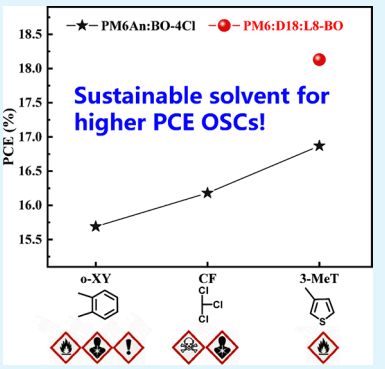

KEYWORDS: *3-methylthiophene, conjugated polymer, organic solar cells, green solvent, sustainable*

1. INTRODUCTION

Solution-processable conjugated polymers are widely used in the fields of solar cells, light-emitting diodes, and field-effect transistors.[1−3] Among them, organic solar cells (OSCs) have the advantages of a simple preparation process, being lightweight and flexible, and having an easy large-area preparation, demonstrating great potential for commercial applications and thus becoming one of the research hotspots in the energy field in recent years.[4−7] Owing to the development of new active layer materials, interfacial layer materials, and new device preparation processes, the field of OSC has made remarkable achievements, and the power conversion efficiency (PCE) has increased from less than 1% to more than 20%, showing excellent development potential and application prospects.[8−12] In the pursuit of developing practical applications for OSCs, it is essential to consider the sustainability of the processes for OSC fabrication, especially the environmental impact of solvents used in the production process, in addition to the PCE.[5,13]

Conjugated polymers tend to exhibit poor solubility due to the strong $\pi-\pi$ stacking of the rigid aromatic backbone; their solubility is generally improved by introducing alkyl chains. In addition, solution processing is achieved by solvents with better solubility such as chloroform (CF), chlorobenzene (CB), and toluene. Solvents such as halogenated hydrocarbons, aromatic hydrocarbons, ethers, amides, etc., which are used as solvents in the preparation of highly efficient OSC active layers in the existing technology, are extremely hazardous to the environment and the human body. For example, solvents such as CF,[14,15] CB,[15−18] and dichlorobenzene,[14,19] which contain halogenated elements, cause serious damage to the ozone layer. Aromatic compounds such as toluene,[20−22] xylene,[23−26] and trimethylbenzene[20,27−29] still have high teratogenic toxicity. Nonaromatic compounds such as tetrahydrofuran[30] and *N*-methylpyrrolidone[31] still have high teratogenic and reproductive toxicity. Some low-toxicity OSC processing solvents have also been reported, e.g., 2-methyltetrahydrofuran,[32−34] anisole,[33,35] carbon disulfide,[36] and D-limonene,[37] but the device efficiency is much lower than other solvents (<16%). Terpene from renewable feedstocks was used to fabricate organic electronic devices such as high-performance OSC light-emitting diodes and field-effect transistors. Due to the poor solubility of terpenes, the addition of highly toxic tetrahydronaphthalene was required to dissolve the conjugated polymers.[2] If these solvents are utilized for large-scale production, then the production process will require strict worker protection and will also result in the emission of large quantities of toxic gases and liquids. These issues will definitely lead to a significant increase in the cost of

Received: July 16, 2024
Revised: August 29, 2024
Accepted: September 6, 2024
Published: September 16, 2024

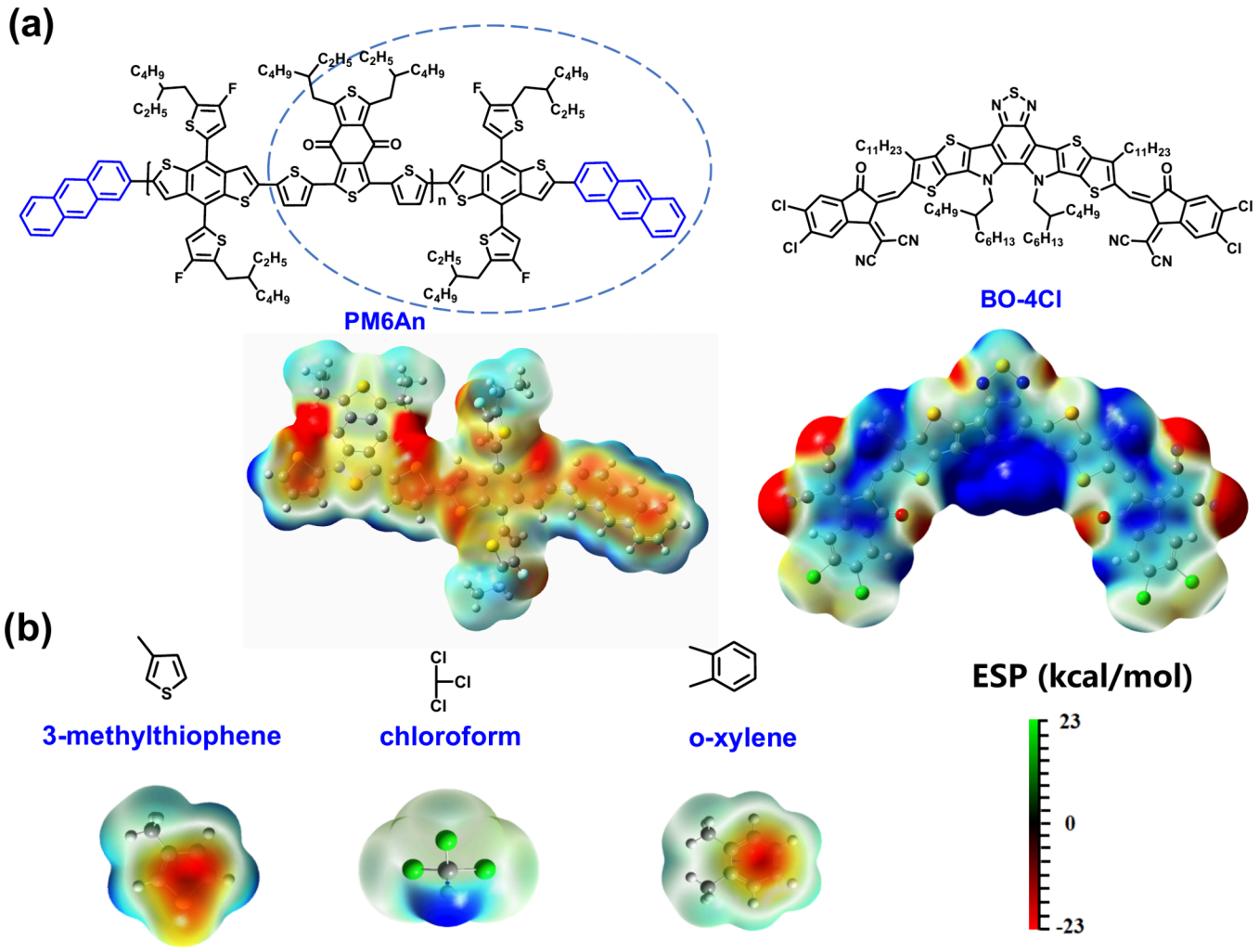

Figure 1. (a) Chemical structures of PM6An and BO-4Cl. Gaussian 09-calculated electrostatic potential of the PM6An end group and BO-4Cl. (b) Chemical structures and electrostatic potentials of 3-MeT, CF, and *o*-XY.

disposal of waste liquids, gases, and solids as well as great damage to human health or the environment. Thus, these seriously limit its large-scale preparation as well as commercial promotion and application.

In addition, the application of water/alcohol solvents for the preparation of OSC active layers has also been reported in some studies.[38] The molecules of water/alcohol-based ecosolvents are strongly polarized, but highly efficient active layer materials usually have weak polarity and strong molecular stacking. According to the theory of like dissolves like, active layer materials have poor solubility in these strong polar environmental solvents, and the photoelectric conversion efficiency of the photoactive materials prepared based on dissolution or dispersion in water or ethanol is generally low. With the help of surfactants, water or alcohol nanoparticle solutions of the active layer can be formed. However, most of these surfactants are insulators and the surface defects of nanoparticles lead to poor photovoltaic performance.[39−45] Further, in order to improve the performance of the active layer material, its solubility or dispersion ability in polar solvents can be improved by introducing strongly polar atoms (oxygen or nitrogen) into the side chains or by employing anionic/cationic surfactants. However, the low oxidation potential of nitrogen atoms traps holes and adversely affects the OSC device performance.[46] Changing the side chains into strongly polar oligo(ethylene glycol) monomethyl ether and other nonionic building blocks not only achieves eco-solvent solubility or dispersion of the conjugated polymers but also has adverse effects on the material's conductivity and device performance.[47−52] Obviously, the photoelectrochemical conversion efficiency is no longer sufficient for the industrialization of OSCs.

Therefore, finding environmentally friendly and low-toxicity organic solvents that can dissolve or disperse conjugated polymers and enhance the performance of the final films is of great value. Currently, the properties of active layers prepared with environmentally friendly and low-toxicity organic solvents do not meet the needs of commercialization. Among them, the molecular electrostatic potential, orientation, and structure of solvents have a significant impact on the morphology of active layer films. Therefore, it is of great significance to study the effects of different organic solvent molecules on the morphology and properties of the films prepared by them and to summarize the constitutive relationship between solvents and the final photovoltaic properties for the development of OSCs.

Based on the theory of like dissolves like, polymer building blocks should dissolve conjugated polymers and small molecules. For example, benzene is one of the common units for organic semiconductors, and its derivatives (toluene,

https://doi.org/10.1021/acsami.4c11805
ACS Appl. Mater. Interfaces 2024, 16, 50916−50925

xylene, and trimethylbenzene) have been used to dissolve active layer materials. Similarly, thiophene and its derivatives should be a potential solvent for polymers. However, they have not been used and recognized as solvents so far.[53−55] Among various thiophene derivatives, 3-methylthiophene (3-MeT) was first chosen because it is cheap and has no poison symbol in its Safety Data Sheet. Here, we have first used 3-MeT to fabricate OSCs with both a higher PCE and lower toxicity than CF or *o*-XY.

2. EXPERIMENTAL METHODS

2.1. Material Synthesis. The PM6An:Tin monomer (200 mg, 0.213 mmol), bromine monomer (190 mg, 0.248 mmol), and 60 mL of dry toluene were added to a dry 100 mL Schlenk bottle. The mixture was purged with nitrogen, and then, $Pd(PPh_3)_4$ (2 mg, 1.73 μmol) was added. The resulting mixture was purged with nitrogen again for 30 min and then stirred at 90 °C for 20 h. After the mixture was cooled to room temperature, tin monomer (66.7 mg, 0.071 mmol) was added to the mixture, and then stirring was continued at 90 °C for 4 h. Pd_2dba_3 (2 mg, 2.18 μmol) and $P(o\text{-tol})_3$ (4 mg, 13.14 μmol) were added to the mixture, followed by 2-bromoanthracene (36.5 mg, 0.142 mmol). The reaction mixture was then heated to 90 °C for 24 h, and then, the temperature was raised to 110 °C to continue the reaction for 24 h. Finally, the reaction mixture was cooled to room temperature, and the product was precipitated using methanol. The black solid was collected by filtration, the polymer was dissolved in CF solvent, and CF was used as an eluent to pass through a coarse silica gel flash column. The polymer solution was rotary-evaporated to remove the solvent and then dropped into methanol. The target copolymer was obtained by filtration and dried in a vacuum oven at 40 °C overnight to obtain a purple-black solid with metallic luster (335 mg, 79%).

2.2. Device Fabrication. Organic photovoltaics were fabricated on glass substrates commercially precoated with a layer of ITO with the conventional structure of ITO/PEDOT:PSS/active layer/PDINN/Ag. Prior to fabrication, the substrates were cleaned using detergent, deionized water, acetone, and isopropanol consecutively for 15 min in each step and then treated in an ultraviolet ozone generator for 15 min before being spin-coated at 3500 rpm with a layer of PEDOT:PSS (Baytron P AI 4083). After baking the PEDOT:PSS layer in air at 150 °C for 15 min, the substrates were transferred to a glovebox. The PM6An:BO-4Cl active layer was spin-coated from a 22 mg/mL 3-MeT solution (D:A = 1:1.2, 50 wt % DIB) at 75 °C and 3500 rpm for 30 s. The PM6An:BO-4Cl active layer was spin-coated from 22 mg/mL *o*-xylene (*o*-XY) solution (D:A = 1:1.2, 50 wt % DIB) at 75 °C and 3500 rpm for 30 s. The PM6An:BO-4Cl active layer was spin-coated from 16.5 mg/mL CF solution (D:A = 1:1.2, 50 wt % DIB) at 3500 rpm for 30 s. The PM6:BO-4Cl active layer was spin-coated from 22.5 mg/mL 3-MeT solution (D:A = 1:1.2, 50 wt % DIB) at 75 °C and 3500 rpm for 30 s. The PM6:L8-BO active layer was spin-coated from 22.5 mg/mL 3-MeT solution (D:A = 1:1.2, 50 wt % DIB) at 75 °C and 3500 rpm for 30 s. The PM6:D18:L8-BO active layer was spin-coated from 22.5 mg/mL 3-MeT solution (D:A = 0.8:0.2:1.2, 50 wt % DIB) at 75 °C and 3500 rpm for 30 s. Then, an extra preannealing step at 100 °C for 10 min was performed. A thin layer of PDINN was spin-coated from 1 mg/mL methanol solution at 4000 rpm for 40 s on the top of the active layer. Finally, the Ag (100 nm) electrode was deposited by thermal evaporation to complete the device with an active area of 6 mm^2, and the testing aperture area was 4 mm^2.

2.3. Computational Details. The ESPs of the molecules were calculated using density functional theory with the B3LYP/6-31G** basis set, and the calculations were performed using Gaussian 09.[56] The ESP statistics of each atom were conducted by using Multifwn.[57]

3. RESULTS AND DISCUSSION

3.1. Solvent Properties. As shown in Figure 1, 3-MeT, CF, and *o*-XY were used to fabricate OSCs based on PM6An:BO-4Cl in this paper. Some physical properties of the solvents are summarized in Table 1. As shown in the table, the boiling point, dipole moment, vapor pressure, and size of 3-MeT are between those of CF and *o*-XY. It should be noted that even though they had been used to fabricate high-performance OSCs, OSCs fabricated by CF usually exhibited higher PCE than *o*-XY in most cases. Thus, we chose 3-MeT because it has a moderate boiling point, vapor pressure, size, and dipole moment between CF and *o*-XY, with the expectation that it may exhibit advantages of both CF and *o*-XY. Compared to *o*-XY, CF has a relatively lower boiling point and higher vapor pressure, which is unsuitable for future large-area printing. It should be noted that 3-MeT had a medium boiling point and vapor pressure, which may exhibit a proper solvent drying time for the active layer. Additionally, the moderate size and dipole moment of 3-MeT may induce an appropriate interaction with donor/acceptor molecules and phase separation. All of these solvents had enough solubility to fabricate OSCs. In addition, the end groups of PM6An, BO-4Cl, and three solvents were simulated by density functional theory, and the corresponding dipole moment and electrostatic distribution were obtained. The dipole moments of the end group of PM6An and BO-4Cl were 0.51 and 0.08 D, respectively. Usually, a larger dipole moment can cause higher relative permittivity and stronger intermolecular interactions.[58] To form proper phase separation within the best exciton diffusion length, the solvent should not be too large or small. 3-MeT has a moderate dipole moment and may interact well with the donor receptor. A higher permittivity can reduce the exciton binding energy and charge recombination loss; strong intermolecular interactions can promote tight packing between molecules, which is beneficial for charge transfer. Thus, it may be a suitable candidate for processing the OSCs. We synthesized an end-capped PM6An according to our previously reported end-capping method.[59] PM6An:BO-4Cl was selected as the active layer to study the photovoltaic properties of OSCs fabricated with different solvents.

Table 1. Boiling Point, Dipole Moment, Vapor Pressure, and Size of the Solvent Molecules

solvent	T_b (°C)[a]	dipole moment (D)	P_{Vapor} (mmHg)[b]	$d_{min} \times d_{max}$ (Å)[c]	S (mg/mL)[d]
3-MeT	115	0.83	23.8	0.40 × 5.57	7.4
CF	61	1.02	197.0	0.51 × 2.93	8.8
o-XY	143	0.57	6.0	0.40 × 5.99	12.8

[a]Boiling point. [b]Measured at 25 °C. [c]Minimum and maximum molecular size. [d]Solubility of PM6An in a solvent.

3.2. Photovoltaic Performance. Then, photovoltaic properties of OSCs fabricated with different solvents or active layers were investigated and are summarized in Table 2 and Figure 2a,b. We have reported that end-capped PM6E7 has a better photovoltaic performance.[59] Based on this, a better end-capped polymer PM6An was synthesized in our lab. Thus, PM6An was first chosen as the donor material due to its high performance and low cost to compare the difference of these solvents. When processed with CF, the PM6An:BO-4Cl-based best device exhibited a moderate V_{oc} of 0.848 V, with a low J_{sc} of 26.52 mA cm^{-2} and FF of 71.99%, all of which contribute to an overall PCE of 16.18%. In going from CF to *o*-XY, the corresponding OSCs showed even worse efficiency (15.69%). When fabricated with 3-MeT, the best device showed a higher

https://doi.org/10.1021/acsami.4c11805
ACS Appl. Mater. Interfaces 2024, 16, 50916−50925

Table 2. Photovoltaic Properties of OSCs Fabricated with Different Solvents and Materials

solvent	D:A	V_{oc} (V)	J_{sc} (mA/cm^2)	FF (%)	PCE[a] (%)
3-MeT	PM6An:BO-4Cl	0.858	26.98	72.91	16.87 (16.70 ± 0.15)
CF	PM6An:BO-4Cl	0.848	26.52	71.99	16.18 (16.00 ± 0.13)
o-XY	PM6An:BO-4Cl	0.843	26.28	70.83	15.69 (15.52 ± 0.24)
3-MeT	PM6:BO-4Cl	0.845	27.22	75.66	17.41 (17.30 ± 0.15)
3-MeT	PM6:L8-BO	0.885	24.93	74.84	16.52 (16.23 ± 0.26)
3-MeT	PM6:D18:L8-BO	0.883	26.91	76.34	18.13 (17.36 ± 0.52)

[a]In parentheses are the average values based on more than eight independent devices.

PCE of 16.87%, with a high J_{sc} of 26.98 mA cm^{-2}, FF of 72.91%, and a reasonable V_{oc} of 0.858 V. The commercial high-performance PM6 was further used to test the universality and photovoltaic performance of 3-MeT for both binary and ternary OSCs. PM6:BO-4Cl and PM6:L8-BO-based best devices showed moderate PCEs of 17.41 and 16.52%, respectively. When the code was changed to PM6:D18:L8-BO, the corresponding best OSC exhibited a remarkable PCE of 18.13% with a relatively high FF of 76.34%.

From the perspective of large-scale production in the future, the extensive use of solvents may cause serious harm to both personnel and the environment. Solvents without toxicity labels in the SDS are potential candidates for addressing pollution. Then, some representative research on polymer solar cells processed with relatively "green and environmental" solvents is summarized in Figure 2c and Table S4. The toxicity of solvents without toxicity labels in the SDS is typically evaluated by using oral-LD50 to assess the degree of toxicity. However, considering that the primary route of exposure to these solvents during the production process is inhalation rather than ingestion, this article employs inhalation LC50 to investigate the toxicity of the solvents. The orl-rat LD 50 and ihl-rat LC50 values of 3-MeT in rats are higher than those of other solvents, indicating that it is more friendly to humans and the environment. It should be noted that due to the relatively high reactivity of β-methyl, S, or α-H in 3-MeT, 3-MeT should be much easier to gather, treat, and dispose of than CF and *o*-XY. To the best of our knowledge, 3-MeT exhibited a relatively high PCE as shown in Figure 2c. In addition, it should be noted that high-performance conjugated polymers such as D18 and PM6 usually have high molecular weights and can only be dissolved in a few solvents. According to literature records, 2-methylanisole, anisole, LM, and eucalyptol cannot dissolve these polymers well. However, 3-MeT has a higher solubility, making it a strong candidate for green and eco-friendly solvents for conjugated polymers.

3.3. Absorption, SCLC Mobilities, and Device Physics. The absorption properties of PM6An, BO-4Cl, and PM6An:-BO-4Cl in thin films were measured and are shown in Figure 2d,e. Obviously, different solvents had different effects on film absorption, especially the BO-4Cl neat films. The PM6An:BO-4Cl film fabricated with 3-MeT showed a slightly higher absorption intensity at some wavelength, which may be because 3-MeT had some effects on the molecular packing. The space charge limiting current (SCLC) method was utilized to calculate the charge transport mobility of films prepared with different solvents. Compared to CF and *o*-XY, both μ_h and μ_e of the active layer film were improved when using 3-MeT, resulting in much more balanced charge transport mobilities (μ_h/μ_e = 1.26).

In order to investigate the charge dissociation and collection process in depth, we further measured the device's photo-generated carrier properties such as the device's photocurrent density ($J_{ph} = J_L - J_D$, where J_L and J_D are the current densities of the device in illumination and darkness, respectively), the effective voltage ($V_{eff} = V_0 - V_{bias}$, where V_0 is the voltage at which J_{ph} is 0 and V_{bias} is the applied bias voltage), the exciton dissociation efficiency (P_{diss}), and the charge collection efficiency (P_{coll}). J_{sat} is mainly the number of photons collected by the active layer, which represents the saturation current density reached when V_{eff} = 2 V. The current density at the short-circuit and the maximum power output conditions are represented by J_{ph}* and $J_{ph}^{\&}$, respectively. Under short-circuit conditions, the exciton dissociation efficiency (P_{diss}) could be calculated by using the formula $P_{diss} = J_{ph}^*/J_{sat}$, and the charge collection efficiency (P_{coll}) could be calculated by using the formula $P_{coll} = J_{ph}^{\&}/J_{sat}$.[60] The P_{diss} and P_{coll} values of OSCs fabricated by 3-MeT were slightly higher than those of CF and *o*-XY, indicating that the thiophene solvent may improve the exciton dissociation and charge collection.[60]

To study the charge recombination of OSC, the light intensity dependence of V_{oc} and J_{sc} was measured. The dependence of J_{sc} on P_{light} can be expressed as $J_{sc} \propto P_{light}^{\alpha}$. As the value of α gets closer to 1, it indicates that bimolecular recombination is inhibited. The relationship equation between V_{oc} and P_{light} was $V_{oc} \propto n((kT/q)\ \ln P_{light}$. The trap-assisted recombination can be completely suppressed when the n value is equal to 1. The α and n values of devices based on 3-MeT, CF, and *o*-XY solvents are 0.941/1.01, 0.937/1.02, and 0.936/1.05, respectively. 3-MeT inhibited both unimolecular recombination and bimolecular recombination in the OSCs, which benefited the enhancement of the efficiency of charge transport and extraction.

TPC and TPV measurements were also performed for different devices. The charge extraction times of the devices with 3-MeT, CF, and *o*-XY are 0.40, 0.60, and 0.68 μs, respectively. Carrier lifetimes are 34.32, 33.91, and 31.11 μs. In general, a relatively shorter charge extraction time and longer recombination lifetime benefited more efficient carrier transport.[61] From 3-MeT to CF or even to *o*-XY, the charge extraction time of their fabricated devices increases, but the recombination lifetime decreases. Thus, using 3-MeT as a solvent to fabricate devices, carrier extraction transport is the fastest and the recombination lifetime is the longest among these solvents, which will result in a 3-MeT-based photovoltaic device with the highest FF.[62]

3.4. Nano Morphology of Blend Films. The morphology of the active layer had a significant effect on the charge carrier transfer/transport and photovoltaic performance. The surface morphology of the hybrid films was probed by atomic force microscopy (AFM). As shown in Figure 3a−c,d−g, the PM6An:BO-4Cl hybrid films processed by 3-MeT and CF exhibited smooth surfaces with root-mean-square (RMS) roughness values of 1.21 and 1.19 nm. When *o*-XY was used,

https://doi.org/10.1021/acsami.4c11805
ACS Appl. Mater. Interfaces 2024, 16, 50916−50925

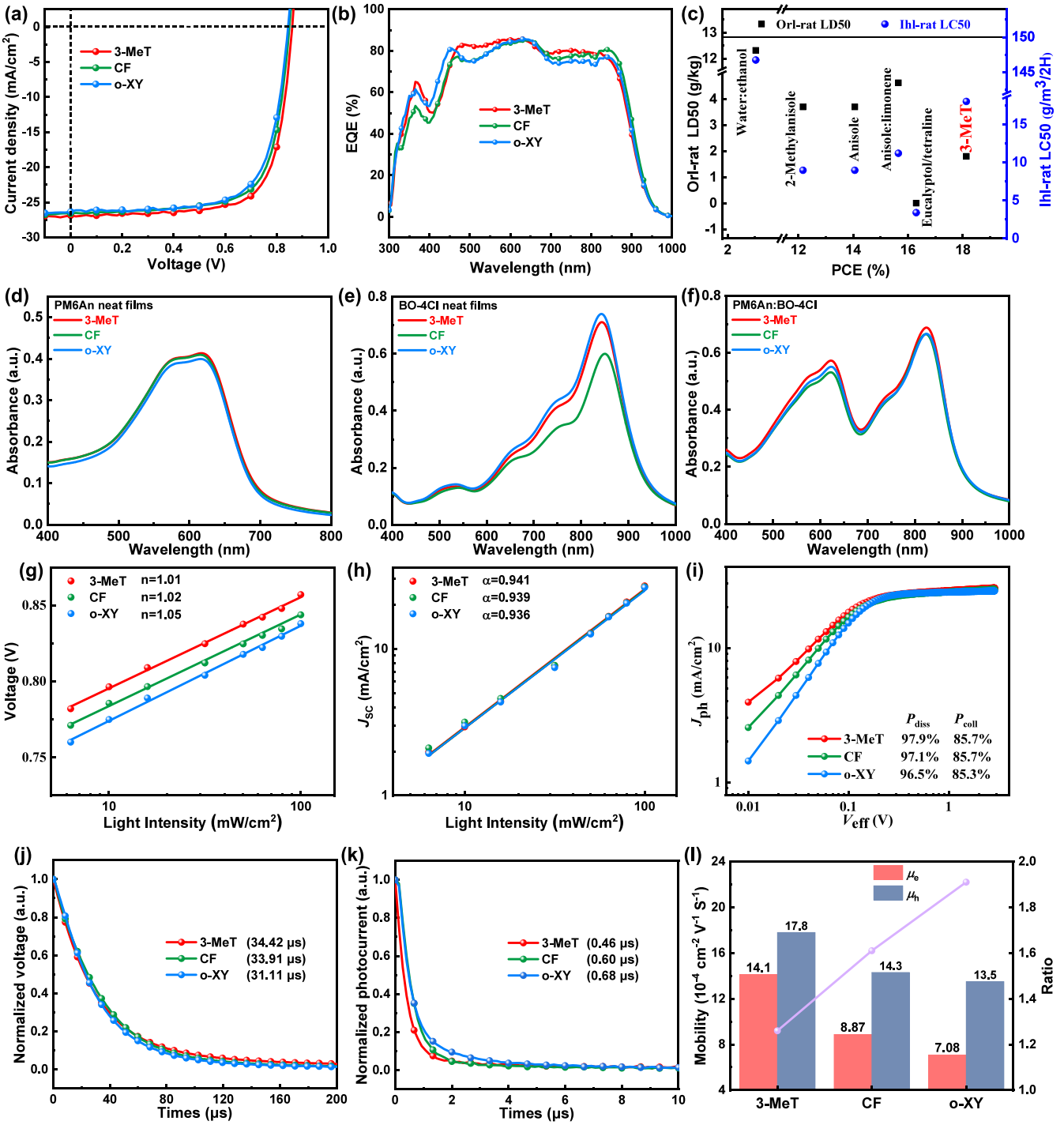

Figure 2. (a) Current−voltage and (b) EQE characteristics of different solvent-processed PM6An:BO-4Cl solar cells under the AM 1.5 condition (100 mW/cm^2). (c) orl-rat LD50 and ihl-rat LC50-PCE of solvents without hazardous symbols in SDS from Sigma-Aldrich. Absorption spectra of (d) PM6An, (e) BO-4Cl, and (f) PM6An:BO-4Cl in thin films. (g) V_{oc} and (h) J_{sc} of the OSC dependence on P_{light}. (i) J_{ph}−V_{eff} curves, (j) transient photocurrent (TPC), (k) transient photovoltage (TPV) measurements, and (l) SCLC mobilities of devices fabricated with 3-MeT, CF, and *o*-XY.

the hybrid films exhibited a slightly enlarged RMS roughness of 1.29 nm. The morphological differences among the three mixtures were also further confirmed by transmission electron microscopy (TEM) measurements. It was clear that the 3-MeT hybrid film exhibits proper phase separation with an improved dark/light contrast, which could be favorable for exciton dissociation and charge transport. In contrast, the films fabricated by CF and *o*-XY tend to have worse phase separation and large grains to some extent. Meanwhile, both the TEM and AFM images indicated that the films fabricated by 3-MeT exhibited a more pronounced fiber interpenetrating network structure, which could be one of the main reasons for the device performance improvement.

Grazing-incidence wide-angle X-ray scattering (GIWAXS) was also performed to investigate the molecular stacking and crystallinity of the active layers. The two-dimensional (2D) GWIAXS images shown in Figure 3i−n, along with the corresponding out-of-plane and in-plane line-cut profiles in

https://doi.org/10.1021/acsami.4c11805
ACS Appl. Mater. Interfaces 2024, 16, 50916−50925

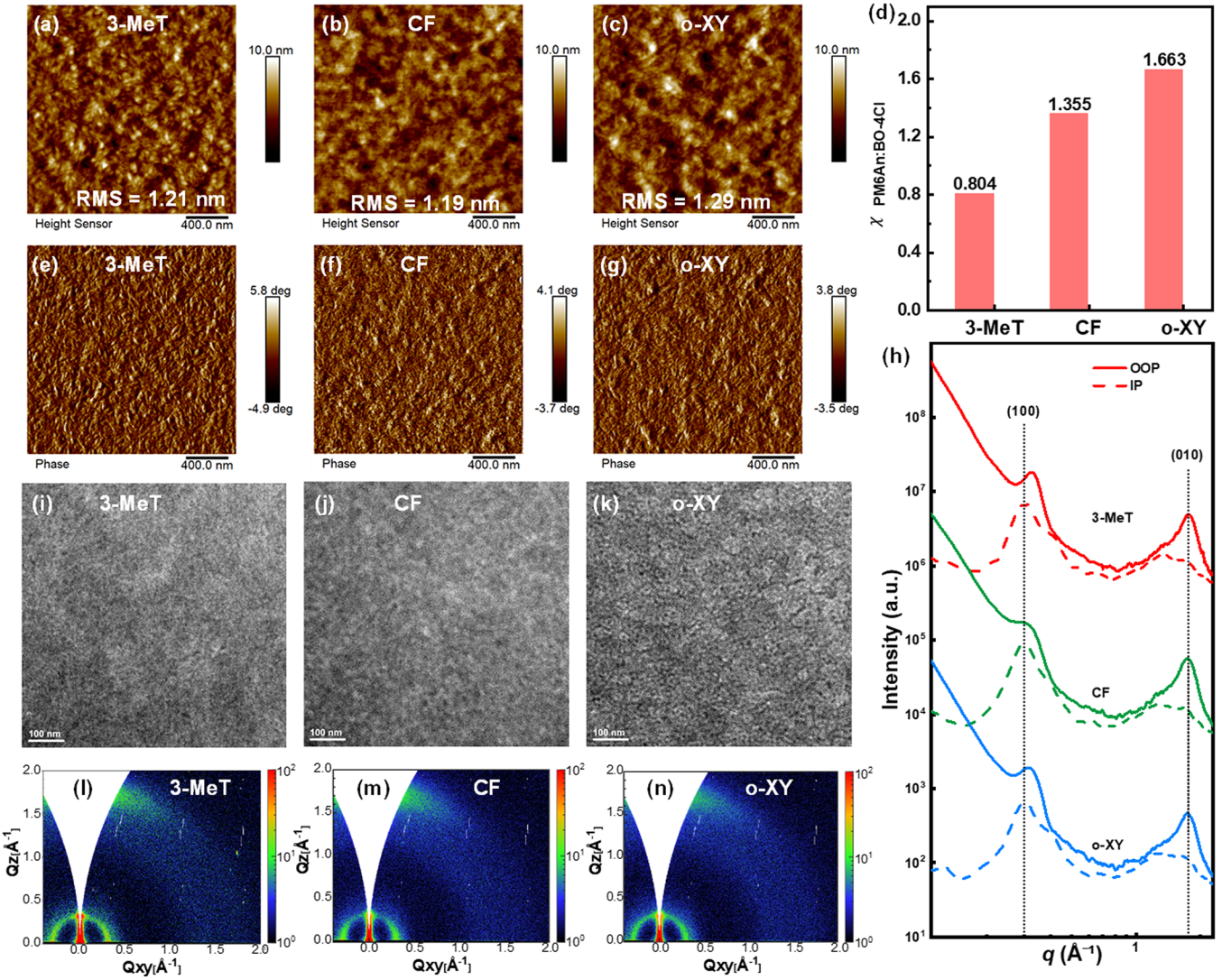

Figure 3. AFM height images of PM6An:BO-4Cl blends fabricated by (a) 3-MeT, (b) CF, and (c) *o*-XY. AFM phase images of the active layer fabricated by (e) 3-MeT, (f) CF, and (g) *o*-XY. (d) PM6An:BO-4Cl interaction parameter with different solvents. TEM images of blend films fabricated by (i) 3-MeT, (j) CF, and (k) *o*-XY. (h) 2D GIWAXS out-of-plane and in-plane scattering profiles for the optimized blend films. 2D GIWAXS patterns of the active layer fabricated by (l) 3-MeT, (m) CF, and (n) *o*-XY.

Figure 3h, and the relevant parameters of the ordered structure of the blend films are provided in Table S3. All films displayed a face-on orientation, characterized by $\pi-\pi$ stacking peaks at around 1.75 $Å^{-1}$ in the out-of-plane (OOP) direction and lamellar stacking peaks at around 0.300 $Å^{-1}$ in the in-plane (IP) direction.[63] As shown in Figure 3, different solvent treatments had a certain impact on the molecular packing in the active layers. The $\pi-\pi$ stacking distances in the out-of-plane (OOP) direction for the active layers treated with 3-MeT, *o*-dichlorobenzene, and CF were 3.57, 3.61, and 3.60 Å, respectively, while the layer stacking distances in the in-plane (IP) direction were 21.02, 21.09, and 21.02 Å, respectively. The active layer treated with 3-MeT exhibited relatively smaller $\pi-\pi$ stacking distances and layer stacking distances. The smaller $\pi-\pi$ stacking distance might have been due to the stronger intermolecular interactions between the receptors after treatment with 3-MeT. The crystal coherence lengths (CCLs) of 3-MeT, CF, and *o*-XY fabricated films in the IP direction were calculated by the Scherrer equation to be 87.3, 85.1, and 84.2 Å, respectively. The change of CCL reflected the crystallinity of the films, which was consistent with corresponding device PCEs. 3-MeT contributed to the highest CCL value, crystallinity, and PCE among these films. These results showed that 3-MeT can effectively control the crystallinity and photovoltaic properties of the active layer. The CCLs of 3-MeT, CF, and *o*-XY blend films in the OOP direction were 19.6, 18.9, and 19.5 Å, respectively. Obviously, the film fabricated by 3-MeT showed better crystallinity in both the OOP and IP directions, which should be the main reason for the improved FF and PCE.

To further study the compatibility between polymer donors and acceptors, the contact angles of different materials with CF, *o*-XY, and 3-MeT in water and ethylene glycol were measured, and the Flory–Huggins interaction parameters were calculated. As shown in Figures 3d, S3, and Table S2, the interaction parameter based on the 3-MeT solvent was the smallest, indicating that the compatibility between the donor and the acceptor should be the best.

https://doi.org/10.1021/acsami.4c11805
ACS Appl. Mater. Interfaces 2024, 16, 50916–50925

4. CONCLUSIONS

In summary, a green and environmentally friendly solvent (3-MeT) was used to fabricate PM6An:BO-4Cl-based OSCs with a reasonable PCE value of 16.87%, which is higher than CF and *o*-XY. Different solvents have various effects on mobility, crystallinity, and morphology. When changed to PM6:D18:L8-BO ternary devices, the highest device fabricated with 3-MeT exhibited a high PCE of 18.13%. 3-MeT exhibits the highest ihl-rat LC50 value among the solvents, which can dissolve conjugated polymers and has no dangerous label in SDS. These results indicated that 3-MeT was a competitive solvent for OSC fabrication, especially for large-scale printing. This research provides an efficient solution for the preparation of OSC reactive layers using environmentally friendly and green solvent treatments and paves an efficient way for large-area printing of OSCs.

■ ASSOCIATED CONTENT

Supporting Information

The Supporting Information is available free of charge at https://pubs.acs.org/doi/10.1021/acsami.4c11805.

Materials; instruments; experimental; device fabrication; NMR measurement; SCLC measurements; contact angle; GIWAXS measurements; some reported OSCs; and toxicity of solvent morphology measurements (PDF)

■ AUTHOR INFORMATION

Corresponding Authors

Meng Wang − *College of Materials Science and Engineering, Hohai University, Nanjing 210098, China; i-Lab & Printable Electronics Research Center, Suzhou Institute of Nano-Tech and Nano-Bionics, Chinese Academy of Sciences, Suzhou 215123, P.R. China;* orcid.org/0000-0003-3607-4071; Email: mwang2021@sinano.ac.cn

Zehua Zhou − *College of Materials Science and Engineering, Hohai University, Nanjing 210098, China;* Email: zhouzehua@hhu.edu.cn

Haiyan He − *College of Materials Science and Engineering, Hohai University, Nanjing 210098, China;* orcid.org/0000-0001-6713-6365; Email: he.haiyan@hhu.edu.cn

Authors

Tingfu Liu − *College of Materials Science and Engineering, Hohai University, Nanjing 210098, China; i-Lab & Printable Electronics Research Center, Suzhou Institute of Nano-Tech and Nano-Bionics, Chinese Academy of Sciences, Suzhou 215123, P.R. China*

Jiaqing Liu − *College of Materials Science and Engineering, Hohai University, Nanjing 210098, China; i-Lab & Printable Electronics Research Center, Suzhou Institute of Nano-Tech and Nano-Bionics, Chinese Academy of Sciences, Suzhou 215123, P.R. China*

Yiming Li − *i-Lab & Printable Electronics Research Center, Suzhou Institute of Nano-Tech and Nano-Bionics, Chinese Academy of Sciences, Suzhou 215123, P.R. China; College of Chemistry and Environmental Science, Key Laboratory of Chemical Biology of Hebei Province, Key Laboratory of Medicinal Chemistry and Molecular Diagnosis, Ministry of Education, Hebei University, Baoding 071002, P.R. China*

Xiaomei Gao − *i-Lab & Printable Electronics Research Center, Suzhou Institute of Nano-Tech and Nano-Bionics, Chinese Academy of Sciences, Suzhou 215123, P.R. China*

Qing Zhang − *Vacuum Interconnected Nanotech Workstation (Nano-X), Suzhou Institute of Nano-Tech and Nano-Bionics of Chinese Academy of Sciences, Suzhou 215123, P.R. China*

Lijun Li − *College of Chemistry and Environmental Science, Key Laboratory of Chemical Biology of Hebei Province, Key Laboratory of Medicinal Chemistry and Molecular Diagnosis, Ministry of Education, Hebei University, Baoding 071002, P.R. China*

Huajie Huang − *College of Materials Science and Engineering, Hohai University, Nanjing 210098, China;* orcid.org/0000-0001-5685-4994

Jinchong Xiao − *College of Chemistry and Environmental Science, Key Laboratory of Chemical Biology of Hebei Province, Key Laboratory of Medicinal Chemistry and Molecular Diagnosis, Ministry of Education, Hebei University, Baoding 071002, P.R. China;* orcid.org/0000-0002-5451-220X

Chang-Qi Ma − *i-Lab & Printable Electronics Research Center, Suzhou Institute of Nano-Tech and Nano-Bionics, Chinese Academy of Sciences, Suzhou 215123, P.R. China;* orcid.org/0000-0002-9293-5027

Complete contact information is available at: https://pubs.acs.org/10.1021/acsami.4c11805

Author Contributions

T.L. and J.L. contributed equally to this work. T.L. and J.L. contributed to data management, formal analysis, investigation, methodology, and manuscript writing. X.G. contributed to software and visualization. Y.L., Q.Z., L.L., H.H., and J.X. contributed to data management and formal analysis M.W., H.H., and Z.Z. contributed to formal analysis, investigation, methodology, writing—review and editing, conceptualization, and funding acquisition. C.M. contributed to resources, supervision, validation, and writing—review and editing.

Notes

The authors declare no competing financial interest.

■ ACKNOWLEDGMENTS

This study was jointly supported by the NSFC (52203249), the Young Innovation Leading Talents of Suzhou Innovation and Entrepreneurship Leading Talents Program (ZXL2022462), and the Suzhou Institute of Nano-Tech and Nano-Bionics, Chinese Academy of Sciences (E1511401). The authors would also like to thank the technical support for Nano-X from the Suzhou Institute of Nano-Tech and Nano-Bionics, Chinese Academy of Science (No. A2107).

■ REFERENCES

(1) Huang, W.; Chen, J.; Yao, Y.; Zheng, D.; Ji, X.; Feng, L.-W.; Moore, D.; Glavin, N. R.; Xie, M.; Chen, Y.; Pankow, R. M.; Surendran, A.; Wang, Z.; Xia, Y.; Bai, L.; Rivnay, J.; Ping, J.; Guo, X.; Cheng, Y.; Marks, T. J.; Facchetti, A. Vertical organic electrochemical transistors for complementary circuits. *Nature* **2023**, *613* (7944), 496−502.

(2) Corzo, D.; Rosas-Villalva, D.; C, A.; Tostado-Blázquez, G.; Alexandre, E. B.; Hernandez, L. H.; Han, J.; Xu, H.; Babics, M.; De Wolf, S.; Baran, D. High-performing organic electronics using terpene green solvents from renewable feedstocks. *Nat. Energy* **2022**, *8* (1), 62−73.

(3) Tang, H.; Liang, Y.; Liu, C.; Hu, Z.; Deng, Y.; Guo, H.; Yu, Z.; Song, A.; Zhao, H.; Zhao, D.; Zhang, Y.; Guo, X.; Pei, J.; Ma, Y.; Cao, Y.; Huang, F. A solution-processed n-type conducting polymer with ultrahigh conductivity. *Nature* **2022**, *611* (7935), 271−277.
(4) Jiang, K.; Zhang, J.; Zhong, C.; Lin, F. R.; Qi, F.; Li, Q.; Peng, Z.; Kaminsky, W.; Jang, S.-H.; Yu, J.; Deng, X.; Hu, H.; Shen, D.; Gao, F.; Ade, H.; Xiao, M.; Zhang, C.; Jen, A. K. Y. Suppressed recombination loss in organic photovoltaics adopting a planar−mixed heterojunction architecture. *Nat. Energy* **2022**, *7* (11), 1076−1086.
(5) Li, H.; Liu, S.; Yao, S.; Wu, X.; Hu, X.; Chen, Y. Advances toward the Device Design and Printing Technology for Eco-friendly Organic Photovoltaics. *Energy Environ. Sci.* **2023**, *16* (1), 76−88.
(6) Zhang, Y.; Deng, J.; Mao, Q.; Young Jeong, S.; Huang, X.; Zhang, L.; Lee, B.; Huang, B.; Young Woo, H.; Yang, C.; Xu, J.; Wu, F.; Cao, Q.-Y.; Chen, L. Facilely full-end-capping engineering promotes high-performance organic solar cells with simultaneously improved efficiency and stability. *Chem. Eng. J.* **2023**, *457*, No. 141343.
(7) Li, B.; Yang, X.; Li, S.; Yuan, J. Stable Block Copolymer Single-material Organic Solar Cells: Progress and Perspective. *Energy Environ. Sci.* **2023**, *16* (3), 723−744.
(8) Wang, J.; Zheng, Z.; Bi, P.; Chen, Z.; Wang, Y.; Liu, X.; Zhang, S.; Hao, X.; Zhang, M.; Li, Y.; Hou, J. Tandem organic solar cells with 20.6% efficiency enabled by reduced voltage losses. *Nat. Sci. Rev.* **2023**, *10* (6), No. nwad085.
(9) Fu, J.; Fong, P. W. K.; Liu, H.; Huang, C.-S.; Lu, X.; Lu, S.; Abdelsamie, M.; Kodalle, T.; Sutter-Fella, C. M.; Yang, Y.; Li, G. 19.31% binary organic solar cell and low non-radiative recombination enabled by non-monotonic intermediate state transition. *Nat. Commun.* **2023**, *14* (1), 1760.
(10) Liu, C.; Fu, Y.; Zhou, J.; Wang, L.; Guo, C.; Cheng, J.; Sun, W.; Chen, C.; Zhou, J.; Liu, D.; Li, W.; Wang, T. Alkoxythiophene-Directed Fibrillization of Polymer Donor for Efficient Organic Solar Cells. *Adv. Mater.* **2024**, *36* (6), No. 2308608.
(11) Sun, Y.; Wang, L.; Guo, C.; Xiao, J.; Liu, C.; Chen, C.; Xia, W.; Gan, Z.; Cheng, J.; Zhou, J.; Liu, D.; Wang, T.; Li, W. π-Extended Nonfullerene Acceptor for Compressed Molecular Packing in Organic Solar Cells To Achieve over 20% Efficiency. *J. Am. Chem. Soc.* **2024**, *146* (17), 12011−12019.
(12) Zhou, J.; Li, D.; Wang, L.; Zhang, X.; Deng, N.; Guo, C.; Chen, C.; Gan, Z.; Liu, C.; Sun, W.; Liu, D.; Li, W.; Li, Z.; Wang, K.; Wang, T. Bicontinuous donor and acceptor fibril networks enable 19.2% efficiency pseudo-bulk heterojunction organic solar cells. *Interdiscip. Mater.* **2023**, *2* (6), 866−875.
(13) Hai, J.; Li, L.; Song, Y.; Liu, X.; Shi, X.; Wang, Z.; Chen, X.; Lu, Z.; Li, X.; Pang, Y.; Yu, J.; Hu, H.; Chen, S. Ending group modulation of asymmetric non-fullerene acceptors enables efficient green solvent processed organic solar cells. *Chem. Eng. J.* **2023**, *462*, No. 142178.
(14) Gao, M.; Zhang, K.; He, C.; Jiang, H.; Li, X.; Qi, Q.; Zhou, K.; Chen, Y.; Zhao, W.; Ye, L. A generic approach yields organic solar cells with enhanced efficiency and thermal stability. *Aggregate* **2023**, *4* (2), No. e289.
(15) Ma, R.; Jiang, X.; Fu, J.; Zhu, T.; Yan, C.; Wu, K.; Müller-Buschbaum, P.; Li, G. Revealing the Underlying Solvent Effect on Film Morphology in High-Efficiency Organic Solar Cells by Combined Ex-situ and In-situ Observations. *Energy Environ. Sci.* **2023**, *16* (5), 2316−2326.
(16) Wang, M.; Cai, D.; Yin, Z.; Chen, S.-C.; Du, C.-F.; Zheng, Q. Asymmetric-Indenothiophene-Based Copolymers for Bulk Heterojunction Solar Cells with 9.14% Efficiency. *Adv. Mater.* **2016**, *28* (17), 3359−3365.
(17) Wan, J.; Zeng, L.; Liao, X.; Chen, Z.; Liu, S.; Zhu, P.; Zhu, H.; Chen, Y. All-Green Solvent-Processed Planar Heterojunction Organic Solar Cells with Outstanding Power Conversion Efficiency of 16%. *Adv. Funct. Mater.* **2022**, *32* (5), No. 2107567.
(18) Ma, R.; Yan, C.; Fong, P. W.-K.; Yu, J.; Liu, H.; Yin, J.; Huang, J.; Lu, X.; Yan, H.; Li, G. In situ and ex situ investigations on ternary strategy and co-solvent effects towards high-efficiency organic solar cells. *Energy Environ. Sci.* **2022**, *15* (6), 2479−2488.
(19) Bai, Q.; Sun, H.; Guo, X.; Niu, L. Advances in Green-Solvent-Processable All-Polymer Solar Cells. *Chin. J. Polym. Sci.* **2022**, *40* (8), 846−860.
(20) Wang, D.; Zhou, G.; Li, Y.; Yan, K.; Zhan, L.; Zhu, H.; Lu, X.; Chen, H.; Li, C.-Z. High-Performance Organic Solar Cells from Non-Halogenated Solvents. *Adv. Funct. Mater.* **2022**, *32* (4), No. 2107827.
(21) Jeon, S. J.; Yang, N. G.; Kim, Y. H.; Yun, J. H.; Moon, D. K. Bihalogenated Thiophene-Based Terpolymers for High-Performance Semitransparent Organic Solar Cells Processed by an Eco-Friendly Solvent and Layer-by-Layer Deposition. *ACS Appl. Mater. Interfaces* **2022**, *14* (33), 38031−38047.
(22) Jeon, S. J.; Yang, N. G.; Kim, J. Y.; Kim, Y. C.; Lee, H. S.; Moon, D. K. A 3-Fluoropyridine Manipulating the Aggregation and Fibril Network of Donor Polymers for Eco-Friendly Solution-Processed Versatile Organic Solar Cells. *Small* **2023**, *19* (38), No. 2301803.
(23) Chen, H.; Zhang, R.; Chen, X.; Zeng, G.; Kobera, L.; Abbrent, S.; Zhang, B.; Chen, W.; Xu, G.; Oh, J.; Kang, S.-H.; Chen, S.; Yang, C.; Brus, J.; Hou, J.; Gao, F.; Li, Y.; Li, Y. A guest-assisted molecular-organization approach for > 17% efficiency organic solar cells using environmentally friendly solvents. *Nat. Energy* **2021**, *6* (11), 1045−1053.
(24) Zhao, H.; Xue, J.; Wu, H.; Lin, B.; Cai, Y.; Zhou, K.; Yun, D.; Tang, Z.; Ma, W. High-Performance Green Thick-Film Ternary Organic Solar Cells Enabled by Crystallinity Regulation. *Adv. Funct. Mater.* **2023**, *33* (5), No. 2210534.
(25) Zhang, J.; Huang, Q.; Zhang, K.; Jia, T.; Jing, J.; Chen, Y.; Li, Y.; Chen, Y.; Lu, X.; Wu, H.; Huang, F.; Cao, Y. Random copolymerization strategy for non-halogenated solvent-processed all-polymer solar cells with a high efficiency of over 17%. *Energy Environ. Sci.* **2022**, *15* (11), 4561−4571.
(26) Wang, H.; Lu, H.; Chen, Y.-N.; Zhang, A.; Liu, Y.; Li, D.; Liu, Y.; Xu, X.; Bo, Z. A Versatile Planar Building Block with C2V Symmetry for High-Performance Non-Halogenated Solvent Processable Polymer Donors. *Adv. Energy Mater.* **2022**, *12* (16), No. 2104028.
(27) Liu, B.; Sun, H.; Lee, J.-W.; Yang, J.; Wang, J.; Li, Y.; Xu, M.; Liao, Q.; Li, B.; Zhang, W.; Han, D.; Niu, L.; Meng, H.; Kim, B.; Guo, X. Achieving Highly Efficient All-Polymer Solar Cells by Green-Solvent-Processing under Ambient Atmosphere. *Energy Environ. Sci.* **2021**, *14* (8), 4499−4507.
(28) Fan, B.; Lin, F.; Oh, J.; Fu, H.; Gao, W.; Fan, Q.; Zhu, Z.; Li, W. J.; Li, N.; Ying, L.; Huang, F.; Yang, C.; Jen, A. K.-Y. Enabling High Efficiency of Hydrocarbon-Solvent Processed Organic Solar Cells through Balanced Charge Generation and Non-Radiative Loss. *Adv. Energy Mater.* **2021**, *11* (41), No. 2101768.
(29) Ma, R.; Yang, T.; Xiao, Y.; Liu, T.; Zhang, G.; Luo, Z.; Li, G.; Lu, X.; Yan, H.; Tang, B. Air-Processed Efficient Organic Solar Cells from Aromatic Hydrocarbon Solvent without Solvent Additive or Post-Treatment: Insights into Solvent Effect on Morphology. *Energy Environ. Mater.* **2022**, *5* (3), 977−985.
(30) Wu, Q.; Yu, Y.; Xia, X.; Gao, Y.; Wang, T.; Sun, R.; Guo, J.; Wang, S.; Xie, G.; Lu, X.; Zhou, E.; Min, J. High-performance organic photovoltaic modules using eco-friendly solvents for various indoor application scenarios. *Joule* **2022**, *6* (9), 2138−2151.
(31) Li, S.; Zhang, H.; Yue, S.; Yu, X.; Zhou, H. Recent advances in non-fullerene organic photovoltaics enabled by green solvent processing. *Nanotechnology* **2022**, *33* (7), No. 072002.
(32) Panidi, J.; Mazzolini, E.; Eisner, F.; Fu, Y.; Furlan, F.; Qiao, Z.; Rimmele, M.; Li, Z.; Lu, X.; Nelson, J.; Durrant, J. R.; Heeney, M.; Gasparini, N. Biorenewable Solvents for High-Performance Organic Solar Cells. *ACS Energy Lett.* **2023**, *8* (7), 3038−3047.
(33) Neu, J.; Samson, S.; Ding, K.; Rech, J. J.; Ade, H.; You, W. Oligo(ethylene glycol) Side Chain Architecture Enables Alcohol-Processable Conjugated Polymers for Organic Solar Cells. *Macromolecules* **2023**, *56* (5), 2092−2103.
(34) Jia, T.; Zhang, J.; Tang, H.; Jia, J.; Zhang, K.; Deng, W.; Dong, S.; Huang, F. Synchronously regulating the alkyl side-chain and regioisomer of polymerized small molecule acceptor enabling highly

https://doi.org/10.1021/acsami.4c11805
ACS Appl. Mater. Interfaces 2024, 16, 50916−50925

efficient all-polymer solar cells processed with non-halogenated solvent. *Chem. Eng. J.* **2022**, *433*, No. 133575.
(35) Pang, S.; Chen, Z.; Li, J.; Chen, Y.; Liu, Z.; Wu, H.; Duan, C.; Huang, F.; Cao, Y. High-Efficiency Organic Solar Cells Processed from Real Green Solvent. *Mater. Horiz.* **2023**, *10* (2), 473−482.
(36) Su, Y.; Ding, Z.; Zhang, R.; Tang, W.; Huang, W.; Wang, Z.; Zhao, K.; Wang, X.; Liu, S.; Li, Y. High-efficiency organic solar cells processed from a halogen-free solvent system. *Sci. China Chem.* **2023**, *66* (8), 2380−2388.
(37) Li, M.-J.; Fan, B.-B.; Zhong, W.-K.; Zeng, Z.-M.-Y.; Xu, J.-K.; Ying, L. Rational Design of Conjugated Polymers for d-Limonene Processed All-polymer Solar Cells with Small Energy Loss. *Chin. J. Polym. Sci.* **2020**, *38* (8), 791−796.
(38) Liu, C.; Liu, J.; Duan, X.; Sun, Y. Green-Processed Non-Fullerene Organic Solar Cells Based on Y-Series Acceptors. *Adv. Sci.* **2023**, *10* (28), No. 2303842.
(39) Xie, C.; Liang, S.; Zhang, G.; Li, S. Water-Processed Organic Solar Cell with Efficiency Exceeding 11%. *Polymers* **2022**, *14* (19), 4229.
(40) Holmes, A.; Deniau, E.; Lartigau-Dagron, C.; Bousquet, A.; Chambon, S.; Holmes, N. P. Review of Waterborne Organic Semiconductor Colloids for Photovoltaics. *ACS Nano* **2021**, *15* (3), 3927−3959.
(41) Xie, C.; Heumüller, T.; Gruber, W.; Tang, X.; Classen, A.; Schuldes, I.; Bidwell, M.; Späth, A.; Fink, R. H.; Unruh, T.; McCulloch, I.; Li, N.; Brabec, C. J. Overcoming efficiency and stability limits in water-processing nanoparticular organic photovoltaics by minimizing microstructure defects. *Nat. Commun.* **2018**, *9* (1), 5335.
(42) Zhang, S.; Zhang, H.; Yang, S.; Zhang, X.; Li, S.; Huang, L.; Jing, Y.-N.; Xiao, L.; Zhang, Y.; Han, B.; Kang, J.-J.; Zhou, H. Synthesis and application of green solvent dispersed organic semiconducting nanoparticles. *Nano Res.* **2023**, *16* (12), 13419−13433.
(43) Kang, S.; Yoon, T. W.; Kim, G.-Y.; Kang, B. Review of Conjugated Polymer Nanoparticles: From Formulation to Applications. *ACS Appl. Nano Mater.* **2022**, *5* (12), 17436−17460.
(44) Du, Y.; Wang, Y.; Shamraienko, V.; Pöschel, K.; Synytska, A. Donor:Acceptor Janus Nanoparticle-Based Films as Photoactive Layers: Control of Assembly and Impact on Performance of Devices. *Small* **2023**, *19* (28), No. 2206907.
(45) Laval, H.; Holmes, A.; Marcus, M. A.; Watts, B.; Bonfante, G.; Schmutz, M.; Deniau, E.; Szymanski, R.; Lartigau-Dagron, C.; Xu, X.; Cairney, J. M.; Hirakawa, K.; Awai, F.; Kubo, T.; Wantz, G.; Bousquet, A.; Holmes, N. P.; Chambon, S. Toward High Efficiency Water Processed Organic Photovoltaics: Controlling the Nanoparticle Morphology with Surface Energies. *Adv. Energy Mater.* **2023**, *13* (26), No. 2300249.
(46) Lee, S.; Jeong, D.; Kim, C.; Lee, C.; Kang, H.; Woo, H. Y.; Kim, B. J. Eco-Friendly Polymer Solar Cells: Advances in Green-Solvent Processing and Material Design. *ACS Nano* **2020**, *14* (11), 14493−14527.
(47) Cui, Y.; Xu, B.; Yang, B.; Yao, H.; Li, S.; Hou, J. A Novel pH Neutral Self-Doped Polymer for Anode Interfacial Layer in Efficient Polymer Solar Cells. *Macromolecules* **2016**, *49* (21), 8126−8133.
(48) Hoang, Q. V.; Song, C. E.; Moon, S.-J.; Lee, S. K.; Lee, J.-C.; Kim, B. J.; Shin, W. S. Asymmetric Electron-Donating 4-Alkyl-8-alkoxybenzo[1,2-b:4,5-b′]dithiophene Unit for Use in High-Efficiency Bulk Heterojunction Polymer Solar Cells. *Macromolecules* **2015**, *48* (12), 3918−3927.
(49) Chang, W.-H.; Gao, J.; Dou, L.; Chen, C.-C.; Liu, Y.; Yang, Y. Side-Chain Tunability via Triple Component Random Copolymerization for Better Photovoltaic Polymers. *Adv. Energy Mater.* **2014**, *4* (4), No. 1300864.
(50) Liu, X.; Xie, B.; Duan, C.; Wang, Z.; Fan, B.; Zhang, K.; Lin, B.; Colberts, F. J. M.; Ma, W.; Janssen, R. A. J.; Huang, F.; Cao, Y. A high dielectric constant non-fullerene acceptor for efficient bulk-heterojunction organic solar cells. *J. Mater. Chem. A* **2018**, *6* (2), 395−403.
(51) Chen, X.; Zhang, Z.; Ding, Z.; Liu, J.; Wang, L. Diketopyrrolopyrrole-based Conjugated Polymers Bearing Branched Oligo(Ethylene Glycol) Side Chains for Photovoltaic Devices. *Angew. Chem., Int. Ed.* **2016**, *55* (35), 10376−10380.
(52) Lee, C.; Lee, H. R.; Choi, J.; Kim, Y.; Nguyen, T. L.; Lee, W.; Gautam, B.; Liu, X.; Zhang, K.; Huang, F.; Oh, J. H.; Woo, H. Y.; Kim, B. J. Efficient and Air-Stable Aqueous-Processed Organic Solar Cells and Transistors: Impact of Water Addition on Processability and Thin-Film Morphologies of Electroactive Materials. *Adv. Energy Mater.* **2018**, *8* (34), No. 1802674.
(53) Byrne, F. P.; Jin, S.; Paggiola, G.; Petchey, T. H. M.; Clark, J. H.; Farmer, T. J.; Hunt, A. J.; McElroy, C.; Sherwood, J. Tools and techniques for solvent selection: green solvent selection guides. *Sustainable Chem. Process.* **2016**, *4* (1), 7.
(54) Henderson, R. K.; Jiménez-González, C.; Constable, D. J. C.; Alston, S. R.; Inglis, G. G. A.; Fisher, G.; Sherwood, J.; Binks, S. P.; Curzons, A. D. Expanding GSK's solvent selection guide−embedding sustainability into solvent selection starting at medicinal chemistry. *Green Chem.* **2011**, *13* (4), 854−862.
(55) Prat, D.; Wells, A.; Hayler, J.; Sneddon, H.; McElroy, C. R.; Abou-Shehada, S.; Dunn, P. J. CHEM21 selection guide of classical- and less classical-solvents. *Green Chem.* **2016**, *18* (1), 288−296.
(56) Frisch, M. J.; Trucks, G. W.; Schlegel, H. B.; Scuseria, G. E.; Robb, M. A.; Cheeseman, J. R.; Scalmani, G.; Barone, V.; Mennucci, B.; Petersson, G. A.; Nakatsuji, H.; Caricato, M.; Li, X.; Hratchian, H. P.; Izmaylov, A. F.; Bloino, J.; Zheng, G.; Sonnenberg, J. L.; Hada, M.; Ehara, M.; Toyota, K.; Fukuda, R.; Hasegawa, J.; Ishida, M.; Nakajima, T.; Honda, Y.; Kitao, O.; Nakai, H.; Vreven, T.; Montgomery, Jr., J. A.; Peralta, J. E.; Ogliaro, F.; Bearpark, M. J.; Heyd, J.; Brothers, E. N.; Kudin, K. N.; Staroverov, V. N.; Kobayashi, R.; Normand, J.; Raghavachari, K.; Rendell, A. P.; Burant, J. C.; Iyengar, S. S.; Tomasi, J.; Cossi, M.; Rega, N.; Millam, N. J.; Klene, M.; Knox, J. E.; Cross, J. B.; Bakken, V.; Adamo, C.; Jaramillo, J.; Gomperts, R.; Stratmann, R. E.; Yazyev, O.; Austin, A. J.; Cammi, R.; Pomelli, C.; Ochterski, J. W.; Martin, R. L.; Morokuma, K.; Zakrzewski, V. G.; Voth, G. A.; Salvador, P.; Dannenberg, J. J.; Dapprich, S.; Daniels, A. D.; Farkas, Ö.; Foresman, J. B.; Ortiz, J. V.; Cioslowski, J.; Fox, D. J. *Gaussian 09*; Gaussian, Inc.: Wallingford, CT, 2009.
(57) Lu, T.; Chen, F. Multiwfn: A multifunctional wavefunction analyzer. *J. Comput. Chem.* **2012**, *33* (5), 580−592.
(58) Gan, Z.; Wang, L.; Cai, J.; Guo, C.; Chen, C.; Li, D.; Fu, Y.; Zhou, B.; Sun, Y.; Liu, C.; Li, W.; Wang, T. Electrostatic force promoted intermolecular stacking of polymer donors toward 19.4% efficiency binary organic solar cells. *Nat. Commun.* **2023**, *14* (1), 6297.
(59) Li, Y.; Liu, J.; Shui, K.; Xie, F.; Li, X.; Lin, Y.; Zhou, Z.; Zhang, Q.; Guo, F.; Li, L.; Xiao, J.; Wang, M.; Ma, C.-Q. Synthesis of Crown Ether End-Capped PM6 Copolymers with Tunable Molecular Weight for Organic Solar Cells. *Macromolecules* **2023**, *56* (16), 6276−6289.
(60) Gasparini, N.; Jiao, X.; Heumueller, T.; Baran, D.; Matt, G. J.; Fladischer, S.; Spiecker, E.; Ade, H.; Brabec, C. J.; Ameri, T. Designing ternary blend bulk heterojunction solar cells with reduced carrier recombination and a fill factor of 77%. *Nat. Energy* **2016**, *1* (9), 16118.
(61) Anitha, B.; Joseph, A.; Alexander, A.; Vijith, K. P.; Varun, S.; Namboothiry, M. A. G. Charge carrier dynamics and photovoltaic properties of near-infrared absorbing squaraine incorporated solution-processed additive-free PTB7:PCBM based ternary solar cells. *J. Phys. D-Appl. Phys.* **2022**, *55* (12), 125301.
(62) Zheng, Y.; Zhao, J.; Liang, H.; Zhao, Z.; Kan, Z. Double-Dipole Induced by Incorporating Nitrogen-Bromine Hybrid Cathode Interlayers Leads to Suppressed Current Leakage and Enhanced Charge Extraction in Non-Fullerene Organic Solar Cells. *Adv. Sci.* **2023**, *10* (26), No. 2302460.
(63) Jiang, X.; Chotard, P.; Luo, K.; Eckmann, F.; Tu, S.; Reus, M. A.; Yin, S.; Reitenbach, J.; Weindl, C. L.; Schwartzkopf, M.; Roth, S. V.; Müller-Buschbaum, P. Revealing donor−acceptor interaction on the printed active layer morphology and the formation kinetics for

https://doi.org/10.1021/acsami.4c11805
ACS Appl. Mater. Interfaces 2024, 16, 50916−50925

nonfullerene organic solar cells at ambient conditions. *Adv. Energy Mater.* **2022**, *12* (14), No. 2103977.

https://doi.org/10.1021/acsami.4c11805
ACS Appl. Mater. Interfaces 2024, 16, 50916−50925